

The Multiple Instances of Node Centrality and their Implications on the Vulnerability of ISP Networks

George Nomikos*

Panagiotis Pantazopoulos*

Merkourios Karaliopoulos[†]

Ioannis Stavrakakis*

* Department of Informatics and Telecommunications
National & Kapodistrian University of Athens
Ilissia, 157 84 Athens, Greece
Email: {gnomikos, ppantaz, ioannis}@di.uoa.gr

[†] Centre for Research and Technology - Hellas
Information Technologies Institute
38334 Volos, Greece
Email: mkaraliopoulos@iti.gr

Abstract—The position of the nodes within a network topology largely determines the level of their involvement in various networking functions. Yet numerous *node centrality indices*, proposed to quantify how central individual nodes are in this respect, yield very different views of their relative significance. Our first contribution in this paper is then an exhaustive survey and categorization of centrality indices along several attributes including the type of information (local vs. global) and processing complexity required for their computation.

We next study the seven most popular of those indices in the context of Internet vulnerability to address issues that remain under-explored in literature so far. First, we carry out a correlation study to assess the consistency of the node rankings those indices generate over ISP router-level topologies. For each pair of indices, we compute the full ranking correlation, which is the standard choice in literature, and the percentage overlap between the k top nodes. Then, we let these rankings guide the removal of highly central nodes and assess the impact on *both* the connectivity properties and traffic-carrying capacity of the network. Our results confirm that the top- k overlap predicts the comparative impact of indices on the network vulnerability better than the full-ranking correlation. Importantly, the locally computed degree centrality index approximates closely the global indices with the most dramatic impact on the traffic-carrying capacity; whereas, its approximative power in terms of connectivity is more topology-dependent.

I. INTRODUCTION

Social Network Analysis (SNA) constitutes a highly interdisciplinary theoretical framework that seeks to process social information and analyze existing social structures [1]. SNA draws heavily on graph models that map individual actors within the social network to the graph vertices and their relationships to the graph (weighted) edges. It then leverages graph-theoretic concepts, metrics and results to answer various questions about the relative importance of the actors for the network or the way that information (or innovations) flow (resp. spread) across it.

The centrality concept, to the best of our knowledge, dates back to the work of Bavelas [2]. By that time significant sociological research was directed to the area of professional

networks addressing how the position and power of individual actors relate to their social interconnections and the way they interact with the rest of the network. Such sociological studies motivated the introduction of various sociological indices, which sought to quantify the *importance* of nodes and their relationships. Bavelas's work appears to be the first to have given a formal definition of node centrality in connected graphs as the sum of its own geodesics (shortest-path distances) to all other nodes.

This work triggered a large research thread and a huge number of publications in the area of centrality indices. Many of them proposed new indices [3] or adaptations of existing ones that expanded their applicability in a broader range of scenarios [4], [5]. The vast majority of work was heuristic and only a few of them attempted to come up with axiomatic definitions of centrality indices and the properties they should satisfy [6]. The highly-cited work of Freeman in [7] appears to have served as a turning point for this first wave of work, by reviewing a number of centrality indices and promoting three of them, *i.e.*, the closeness, degree, and betweenness, as the most representative ones. About the same time Bonacich had established the eigenvector centrality as a fourth, distinctly different but equally popular, index [8].

The research interest in the centrality concept revives in late 90's and early 2000, primarily through the works of physicists such as D. Watts and M. Newman. They use centrality indices to explore the vulnerability and community structure, respectively, of general network instances. SNA techniques and centrality, in particular, find applicability to research work across a broader set of disciplines beyond sociology. In the case of computer scientists, insights from centrality indices are primarily exploited in the design of more effective protocols for communication networks [9], [10]. The trend is only catalyzed by the broader expectations about the evolution of a *Network Science* [11], which could serve as the theoretical foundation for a unified treatment of all network types.

Motivation and objective: The relevance of centrality indices to the communication network (*i.e.*, Internet topologies) robustness, in particular, is the motivation for this study. Our main objective is to *quantify how much information is embedded in centrality indices about the relative importance*

[†] The major part of this work was carried out while Dr. Karaliopoulos was affiliated with the Department of Informatics and Telecommunications, UoA. This work has been partially supported by EINS, the Network of Excellence in Internet Science through EC's Grant Agreement FP7-ICT-288021.

of Internet nodes for different network operations. Given that the different formulations of centrality proposed in literature are heuristic, the questions that naturally arise are how do these formulations compare in their assessments/predictions about the relative importance of network nodes and which one(s) may be the “right one(s)” to consider as reference for more reliable predictions of network robustness.

The paper seeks to *systematically* address these questions by undertaking a three-step study with various instances of methodological innovation. The first step involves a thorough survey and novel classification of the variety of centrality indices proposed in literature over the last sixty years. This classification is then used to select the seven most popular and representative indices for carrying out the two experimental steps of the study. Hence, as a second step, we derive the node rankings these indices induce over more than 40 *router-level* snapshots of network topologies and study their correlation. The correlation strength is assessed by the mainstream rank/linear correlation coefficients but also less widespread measures such as the percentage overlap in the lists of the k most central nodes. Finally, we compare the seven indices with respect to their capacity to reveal the network vulnerability to node removals; we let the indices dictate the most central nodes to-be-removed and assess how the *network connectivity* properties but also its *traffic-carrying capacity* are affected.

Our results identify certain index pairs with consistently high full rank correlation across all datasets we experiment with. However, they also warn against the interpretation of its high values showing that significant part of this correlation is due to nodes at the bottom of the rankings. As a result, the percentage overlap of the k most central nodes for the same pairs assumes clearly smaller values. Among the noteworthy results is that when the nodes removals are driven by the single index that can be computed through local-only information (*i.e.*, the Degree Centrality index), the impact on the network traffic serving capacity approximates closely the maximum over the seven indices. The hint for network vulnerability studies is that the added complexity of global indices may be circumvented when an estimate of what is the worst-case impact on the network is needed.

The remainder of the article is structured as follows: In Section II, we summarize a survey of a broad range of proposed centrality indices over the last sixty years and the classification scheme we adopted. Note that a detailed description of the various centrality formulations appears in [12]. We then turn to the question of how much information different centrality indices entail regarding the importance of network nodes and the resulting network vulnerability. First, we select a subset of seven popular indices and carry out a correlation study in Section III. Then, in Section IV we let the seven indices drive targeted node attacks over the Internet graphs and experimentally assess their impact in both connectivity and traffic-carrying capacity terms. Related literature is summarized in Section V. Finally, we conclude the paper with a summary of the main messages out of our study in VI.

II. A NOVEL CLASSIFICATION OF CENTRALITY INDICES

In this report, we attempt to summarize this classification, pointing the interested reader to [12] for a much more detailed description of the indices and the context within which they were originally proposed. At a first-level the reviewed indices are split between *node* (point) centrality and *graph* centrality indices. The former, which are addressed by the vast majority of the literature, characterize individual nodes, whereas the latter are derived for whole graphs as functions of the individual node centrality indices. Then, node centrality indices are further characterized in line with the attributes shown in Fig. 1. These include the network properties that are reflected in the index formulation (topological *vs.* flow-aware), the type of underlying graph over which an index is computed, as well as computational aspects such as the amount of information (local *vs.* global) and complexity involved in the index computation.

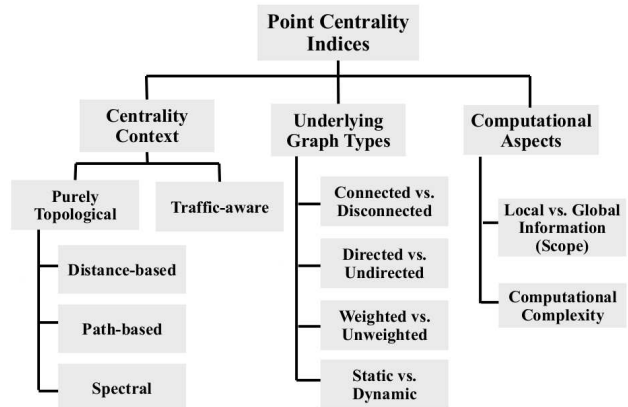


Fig. 1. Classification tree of point centrality indices.

A. Node centrality indices

The first broad category groups point centrality indices that have been, at least originally, proposed for connected, binary, non-directed graphs.

1) Context: Purely topological *vs.* flow-aware:

a) *Pure topological indices*: This set of centrality indices takes into account only the network topology, *i.e.*, the nodes and the links between them. Topological indices may reflect two different aspects of a node’s position in a network.

Distance-based centrality: The corresponding indices measure how distant a node is from all other network nodes. Indices that fall in this category are the Closeness Centrality [7] and Eccentricity [13].

Path-based centrality: Indices of this type assess to what extent a node lies on *paths* connecting other nodes in the network. Degree and Betweenness Centrality are some of the relevant indices [7].

Both types of indices can be further differentiated as to whether the distance (resp. path) definition accounts only for geodesics (*i.e.*, shortest paths) between node pairs or a broader set of paths connecting them. Therefore, indices such as the

Katz index [3] and random walk betweenness [14] essentially relax the underlying assumption that information flows only through shortest path routes.

A third category of topological indices, which has been shown to be closely related to path-based centrality, are spectral centrality indices. Common to these indices are their dependence on the eigenstructure of a matrix related to the network in question and their computation through linear-algebraic manipulations. The indices, sometimes also called “prestige” measures of centrality [1], have the special feature that the centrality index of a node is a function of the centralities of the nodes it is (directly) connected to. The eigenvector centrality index [8] is the most popular one in this family.

b) Flow-aware indices: The so far considered centrality indices rank the graph nodes taking into account the network topology only. A separate thread of work has attempted to factor the traffic that a network is expected to serve in the computation of the centrality indices. The traffic-aware betweenness [15] and the weighted conditional betweenness centrality [16] are two relevant indices.

2) Underlying graph types: Most, if not all, of the considered centrality indices are defined over *connected, undirected, binary, static* graphs. In what follows, we relax in turn each one of these four graph attributes and discuss how the centrality indices are adapted to the resulting types of graphs.

a) extensions of centrality indices for disconnected graphs: Most of the centrality metrics have been formulated and proposed with connected networks in mind, *i.e.*, there are finite paths between every pair of nodes in the network that together form a single giant connected component. Much less attention has been paid to centrality metric formulations for disconnected graphs featuring more than one connected component and/or isolated nodes. Notably, some metric definitions are such that they can directly generalize for disconnected graphs without any additional care. For instance, this is the case with the degree and betweenness centrality while the closeness centrality metric as defined by Beauchamp [4] and Freeman [17] does not trivially generalize into disconnected graphs.

b) extensions of centrality indices for directed graphs: The main body of work that proposes centrality indices appropriate for directed graphs, evolves around the spectral ones. PageRank, one of the most discussed implementation on the Web, delineates the basic model to effectively manage graph-based structures composed by directed (either inbound or outbound) links [18].

c) extensions of centrality indices for weighted graphs: Adaptations of centrality metrics for weighted graphs have been mainly proposed for the three most common centrality indices, the Degree, Betweenness and Closeness Centrality; in the last two instances, only geodesics are considered. The intuitive way to expand the node degree centrality definition is by replacing the sum of the node’s neighboring links with the sum of their weights [19]. Likewise, the notion of link distance (or cost) underlying both the betweenness and

closeness centrality indices is captured by its (inverse) weight and geodesics are estimated accordingly [20].

Regarding spectral indices, to derive the Eigenvector centrality variant for weighted graphs it suffices to substitute the binary elements of the adjacency matrix involved in the eigenvector computations with the edge weights [21]. The extension of PageRank is somewhat more involved; the index originally designed to rank Web pages exploits the binary graph based nature of the Web. However, treating equally all inbound and outbound links remains restrictive when measuring the importance of each page. Therefore, proposed extensions of PageRank over weighted networks assign to each outlink page a value proportional to its popularity [22] or use factors to modulate how rank scores are distributed to neighbors [23], [24]. With hyperlink weights, the surfer can now express preferences among pages instead of uniformly jumping to arbitrary ones.

d) extensions of centrality indices for dynamic graphs: The extension of standard complex network indices, including centrality ones, to networks that vary over time is a more recent thread. There are more than one graph representations for dynamic networks and many more terms that are used to denote them such as temporal graphs [25], evolving graphs [26], space-time graphs [27] or time-varying graphs [28]. To the best of our knowledge, there have been two main studies that have proposed adaptations of centrality indices for temporal graphs. The first one draws on the notion of temporal path [29] over a sequence of graph instances, whereas the second relies on a time-expanded graph representation to define temporal Betweenness and Closeness indices [30].

3) Computational Aspects:

a) Index scope (local vs. global): Centrality indices can be separated into local and global ones, depending on the extent of topological information that is required to compute them. For instance, since Degree Centrality is a function of the number of direct (one-hop) neighbors, it is a local index. On the other hand, Betweenness and Closeness Centrality are global indices in that they rely on geodesic paths computed all over the network.

One typical way to control the scope of (path-based) centrality computations is through the sociological notion of the ego-network. The ego network of a node v is the subgraph involving v , called the “ego” node, its 1-hop neighbors, and their inter-connections. The ego network (centered-graph [31] in graph theoretic terms) is used sometimes to derive a local approximation of an otherwise global centrality index. Betweenness Centrality is a typical index that lends to ego-centric approximations [32]. Another way to control the scope of centrality indices, this time purely path-based indices, is by controlling the length k of paths that are taken into account in their computation. Indices such as k -path [33] and vertex-disjoint k -path centrality [34] are examples of this category.

b) Computational cost of the index: Of particular interest for embedding centrality indices in communication network protocols is their computational complexity. The centrality interpretation by Freeman [17] does not seem to require special

TABLE I
PROPERTIES OF SEVEN POPULAR CENTRALITY INDICES UNDER A NOVEL CLASSIFICATION SCHEME

Centrality Index	Context			Type of underlying graph							Computational aspects		Definition	
	Topology aware			Binary/weighted		Directed/Undirected		Dynamic	Connected/Disconnected		Information (local/global)			Complexity
	path	distance	spectral	B	W	D	U	D	C	D	L	G		
Betweenness (BC)	✓			✓	✓	✓	✓	✓	✓	✓		✓	$O(V E)$	$c_i^{BC} = \frac{2}{(N-1)(N-2)} \sum_{j \neq k \neq i} \frac{d_{i,k}^{(i)}}{d_{j,k}}$
Closeness (CC)		✓		✓	✓	✓	✓	✓	✓	✓		✓	$O(V(\log V) E)$	$c_i^{CC} = \frac{N-1}{\sum_{j \in G, j \neq i} d_{i,j}}$
Degree (DC)	✓			✓	✓	✓	✓	✓	✓	✓	✓	✓	$O(V^2)$	$c_i^{DC} = \frac{deg(i)}{N-1}$
Eccentricity (ECC)		✓		✓	✓	✓	✓	✓	✓	✓		✓	$O(V(\log V) E)$	$c_i^{ECC} = \frac{1}{max_{j \in V} d_{i,j}}$
Eigenvector (EC)			✓	✓	✓	✓	✓	✓	✓	✓		✓	$O(V^3)$	$c_i^{EC} = \frac{1}{\lambda} \sum_{j \in G} \alpha_{i,j} \cdot c_j^{EC}$
Harmonic (HC)		✓		✓	✓	✓	✓	✓	✓	✓		✓	$O(V(\log V) E)$	$c_i^{HC} = \frac{1}{N-1} \sum_{j \in G, j \neq i} \frac{1}{d_{i,j}}$
PageRank (PG)			✓	✓	✓	✓	✓	✓	✓	✓		✓	$\Omega(\frac{E^2}{ln(1/(1-d))})$	$c_i^{PG} = \frac{1-d}{N} + d \sum_{v \in B_i} \frac{c_v^{PG}}{L_v}$

N : Total number of nodes, $d_{i,j}$: Shortest path length from i to j , $d_{j,k}^{(i)}$: Shortest path length via k , $\alpha_{i,j}$: Adjacency matrix element d : Damping factor, B_i : Set of nodes linked to i , L_v : Out-degree of node v

computing power to be applied on large network structures. On the contrary, the solution proposed by Bonacich [35] to correlate the point centralities with graph centralities, could be considered computationally heavy as the network size increases. Consequently, he suggested a way to control this limitation using a new kind of matrix known as “overlapping” instead of adjacency matrix before the eigenvector calculation. Also, Moxleys’ solution [36] for (un)connected graphs seems to encounter the same serious problem with their AIC (Adjusted Index of Centrality) metric when analyzing rich datasets. As a result, they managed to represent the connections of each element in a vector based structure to efficiently compute the adjacency matrix and measuring the centrality for every reached or unreached point.

B. Graph centrality indices

Centrality indices have also been proposed as single numbers for the whole graph (*i.e.*, graph centrality indices). If point centrality indices essentially generate rankings of nodes within a given graph, graph centrality indices seek to rank different graphs. Note that the first studies on point centrality indices by Bavelas [2] and Beauchamp [4] address graph centrality indices as well. Graph centrality was initially defined as the sum of point centralities over each network node. Later on, more complex axiomatic definitions appeared in literature (*e.g.*, [6]), therefore assigning different notions to the graph centrality indices. A more insightful categorization attempt is given by Høivik [37] and recognizes three graph centrality concepts:

1) *Integration*: This is a measure of how centrally located are the nodes of a graph as a whole. It is measured by the sum of individual node centrality indices. This is what Freeman calls *compactness* in his definitions of graph centrality indices out of the Degree, Betweenness and Closeness Centrality indices [7].

2) *Unipolarity*: Reflects whether there is a very central node and is taken equal to the maximum node centrality.

3) *Centralization*: Captures the dispersion of the node centrality values and is taken equal to the sum of differences of point centralities from the minimum point centrality value.

As a final note, the interpretations of centrality indices are multiple. To refer to some of those, Freeman noted that central parties may generally affect the communication, facilitating or even distorting whatever flows in the network. Particularly, from the perspective of degree centrality, he argued that a point with relative high degree serves to control the communication activity inside the topology having the advantage of binding together flow processes [12]. Bonacich agreed saying that a central firm has the possibility to acquire satisfying information rapidly and therefore with high probability. Borgatti on the other hand, tried to shed more light on the question of which centrality index is appropriate for which occasion [38]. He introduced general flow typologies over networks using two criteria *i.e.*, the way the flow is realized in the network (*i.e.*, point-to-point transfer, serial and parallel duplication) and the kind of graph-theoretic path (*i.e.*, walk, trail, and path) that is relevant.

C. Selecting centrality indices for experimentation

In summary, the survey work in this Section has shown that there is a plethora of centrality index formulations, many of them capturing different properties of network nodes. For the experimentation that follows, we select seven indices that include the most popular ones, *i.e.*, those that are repeatedly considered in the literature, and, at the same time, are highly representative of the attributes discussed in the survey: the Degree (DC) [7], Betweenness (BC) [7], Closeness (CC) [7], Eigenvector (EC) [8], Harmonic Centrality (HC) [39], Pagerank (PG, with the damping factor d set to 0.85 as typically used in literature) [18] and Eccentricity (ECC) [13].

In Table I we characterize them according to the aforementioned classification attributes. Also the formal normalized definitions are recalled for each index along with the running time of the algorithms utilized for their computation, as function of the node V and edge E sets of a graph $G = (V, E)$.

III. CORRELATION STUDY OF CENTRALITY INDICES

In almost all instances, where centrality indices inform communication network protocols, what matters is the *ranking* of nodes that is induced by the indices rather than the absolute centrality values. These rankings are subsequently used in

the decisions made by the respective protocols. For example, in [9], [40], the rankings determine whether a Delay Tolerant Network (DTN) node will forward a message to another DTN node it encounters; in [10], whether a content item will be cached at a Information-Centric Networking (ICN) node or not; and in [41] whether to search for a file in a given unstructured Peer-to-Peer(P2P) network node or not. Likewise, in vulnerability analysis of the service migration protocol in [16], it is the *set* of the k , $k < |V|$ most highly-ranked nodes that matters, again irrespective of their actual centrality values. The question that plausibly arises in every case is how similar are the rankings generated by each centrality index.

In this section, we carry out a thorough correlation study of these rankings, as computed over a broad set of ISP router-level topologies. The study proceeds in two steps. First, (**Step 1**) we calculate for each network topology and each node in it the seven centrality index (see subsection II-C) values, thus generating seven different node rankings per topology. Then, (**Step 2**) we compute pairwise correlation measures over these rankings. Two different measures are considered, one accounting for the full node rankings and the other only for the highly-ranked nodes.

A. Index correlation measures and router-level topologies

1) *Index correlation measures*: The first correlation measure is the nonparametric Spearman’s rank-correlation coefficient, ρ , and is computed over the full node rankings. The coefficient assesses how well a monotonic function can describe the rankings induced by the two centrality indices on the network nodes. For a given network topology node set V , it is given by:

$$\rho_V(C_1, C_2) = 1 - \frac{6 \sum_{u \in V} (r_{C_1}(u) - r_{C_2}(u))^2}{|V|(|V|^2 - 1)}$$

where $r_{C_1}(u)$ and $r_{C_2}(u)$ are the ranks of node u in line with centrality indices C_1 and C_2 , respectively. The coefficient values lie in $[-1, 1]$, with high positive (negative) values denoting strong positive (resp. negative) correlation¹.

The second correlation measure is the percentage overlap between the sets of the k most highly ranked (top- k) nodes that are generated by two centrality indices.

$$ov_V(C_1, C_2; k) = \frac{|\{v \in V : r_{C_1}(v) \leq k\} \cap \{v \in V : r_{C_2}(v) \leq k\}|}{k} \cdot 100\%$$

Contrary to the Spearman’s coefficient, the percentage overlap is computed over a subset of the full node rankings and takes values in $[0, 100]$.

¹We have also computed the other popular rank-correlation coefficient, Kendall’s τ . In general, these two non-parametric coefficients, Spearman’s and Kendall’s, produce similar results, as will be reported later in Figure 2 and in more details in the Appendix. Finally, for the sake of completeness we have also computed the well-known Pearson coefficient r that assesses how linear is the relationship between the actual values of the indices rather than the rankings they induce. Typically, the highly rank-correlated centrality pairs have also been found to exhibit considerable linear correlation, yet of lower strength [12].

The relevance of the two measures depends on the usage context of centrality-based ranks. The decisions that relate to the DTN forwarding, CCN caching and P2P node search examples rely on full node rankings; whereas, vulnerability analysis is usually concerned with the subset of nodes that are important (“central”) for the network. High correlation between the rankings of two indices implies that a computationally complex or intractable index can be approximated by a simpler one without significant penalties for the intended protocol operation or the conclusions of the vulnerability analysis.

2) *Router-level ISP topologies*: All experiments in this paper are carried out over datasets collected in the context of four projects. Four of them relate to measurement projects and are referred to as Rocketfuel [42], CAIDA [43], and mrinfo (Tier-1 and Transit) [44] datasets, respectively. They report *binary* router-level graphs² for different Internet ASes. On the contrary, the last dataset, called the Topology Zoo dataset, contains *capacitated* topologies at the router- and Point-of-Presence (PoP) level [46], as collected directly by network operators of primarily academic and research networks. The basic properties of the all datasets are summarized in Tables VI and VII in the Appendix.

a) *Rocketfuel dataset*: The Rocketfuel dataset [42] is the chronologically oldest dataset, drawn with the help of the `traceroute` active measurement tool. The Rocketfuel engine collected raw `traceroute` data from public BGP tables, processed them and extracted router-level networks by mapping diverse ISP routers to ASes. Ten diverse ISPs across the world were mapped utilizing approximately 800 `traceroute` sources hosted by nearly 300 servers.

b) *CAIDA dataset*: CAIDA topologies (IDTK 2011-10) [43], the most recent release out of our datasets, were obtained by means of an active measurement infrastructure known as Archipelago; it performed `traceroute` probes to randomly-chosen destinations, located in 29 countries worldwide within the interval of Oct 24 to Nov 3, 2011. At first, publicly available BGP dumps were used to map IP addresses to ASes relying on several tools for alias resolution. Then, heuristic rules [43] properly assigned each router to the AS it belongs.

c) *Mrinfo datasets*: The Mrinfo [44], dataset was collected during the period 2005-2008 and contains 264 Tier-1, 244 Transit, and 342 Stub ISP network topology files. To cope with `traceroute` inaccuracies, the dataset collection was extracted by the new `mrinfo` tool which silently crawls IPv4 addresses only, based on the Internet Group Management Protocol (IGMP). The advantage of this tool is twofold; it can efficiently discriminate interconnections between ASes without suffering from IP alias resolution problems and, besides layer-3 devices, detect the presence of level-2 hardware (switches) between interconnections of routers for each AS. In our study we considered only the largest available snapshots

²Many of the original network topology files, as released in a raw trace-based format, miss some edges. We have therefore used a wellknown linear-time algorithm [45] to retrieve the giant connected component (GCC).

corresponding to two datasets, Tier-1 and Transit, leaving aside the small-sized Stub topologies.

d) *Topology Zoo dataset*: Whereas previous studies employ a number of route discovery tools to reveal the Internet connectivity, the Topology Zoo gathers the maps of more than 140 real-world topologies directly from the network operators, including layout views of the optical fibers used for both commercial (COM) and Research & Education (REN) networks. As the resulting maps (topologies and associated attributes) come from the owner and/or manager of the network, they are claimed to reflect an accurate network view circumventing any errors due to biases of measurement techniques. Out of the 232 network graphs included in the Zoo, we have carefully singled-out the largest capacitated router-level snapshots (see Table VII in the Appendix) representing the topologies³ of 11 different European, one Asian and one cross-European research networks as traced during the period 2008-2011. We will use these topologies to evaluate the traffic-serving capacity of networks (see Section IV-B).

B. Results

1) *Full-ranking correlation over binary graphs*: The results follow a similar trend over the four datasets so that the rank correlation between the studied indices can be summarized in the graphs of Fig. 2. This graph-based illustration represents all AS topologies⁴ since they exhibit similar coefficient values for every distinct centrality pair. Notably, none of the possible centrality pairs have been found to be negatively correlated over any of the studied topologies. With this in mind, we empirically characterize the correlation strength as *high* and *low* when the corresponding coefficient exhibits a value in the interval $[0.7, 1]$ and $[0.3, 0.7)$, respectively; the two indices are actually uncorrelated when coefficients lie in $[0, 0.3)$. Accordingly, bold edge-lines (solid or dashed) denote high correlation values between two centralities, whereas plain edge-lines denote low values. We have omitted the connections for those index pairs that do not exhibit any kind of correlation.

In what follows, index pairs of interest are discussed in more detail. Where appropriate we draw links to studies reporting similar or different results on different kinds of networks. In Table II each row (*i.e.*, top to bottom) in every box reports averages measured over the CAIDA, Rocketfuel, MrInfo - Tier1 and -Transit datasets, respectively. The interested reader is referred to [12] for the full set of results while in the Appendix (*i.e.*, Table VIII) she can find the respective table when the Kendall τ is used as correlation measure.

Betweenness vs. Degree centrality Degree centrality (DC) captures, at least phenomenally, a completely different notion

³Especially for Uninett I and II networks, there are three snapshots of the same topology but with different link capacities; the original Uninett networks have a couple of links which are tagged with capacities given in min-max format and therefore we have reproduced the three snapshots by taking the minimum, maximum and mean value of the given capacity interval.

⁴The summarizing graphs have been derived considering the corresponding averages of every coefficient for each dataset. The relevant Kendall coefficient and top-5% overlap averages (per dataset) appear, respectively, in Table VIII and IX of the Appendix.

TABLE II
AVERAGES OF SPEARMAN COEFFICIENTS FOR ALL DATASETS

	CC	HC	EC	ECC	DC	BC	PG	dataset
CC	1							CAIDA
	1							RocketFuel
	1							MrInfo-Tier1
	1							MrInfo-Transit
HC	0.99	1						-/-
	0.98	1						
	0.95	1						
	0.99	1						
EC	0.93	0.95	1					-/-
	0.80	0.83	1					
	0.66	0.69	1					
	0.86	0.88	1					
ECC	0.84	0.84	0.84	1				-/-
	0.73	0.67	0.56	1				
	0.80	0.69	0.52	1				
	0.89	0.88	0.75	1				
DC	0.28	0.28	0.29	0.25	1			-/-
	0.48	0.53	0.45	0.38	1			
	0.43	0.59	0.47	0.30	1			
	0.50	0.55	0.49	0.45	1			
BC	0.29	0.29	0.28	0.27	0.90	1		-/-
	0.45	0.50	0.40	0.37	0.94	1		
	0.50	0.61	0.30	0.38	0.69	1		
	0.54	0.58	0.48	0.47	0.88	1		
PG	0.04	0.05	0.05	0.04	0.86	0.80	1	-/-
	0.25	0.30	0.14	0.20	0.83	0.80	1	
	0.34	0.49	0.30	0.24	0.90	0.74	1	
	0.40	0.44	0.36	0.35	0.92	0.88	1	

of centrality than Betweenness (BC). DC takes into account only the node's local neighbors, whereas BC considers the position of the node within the whole network. Therefore, in some cases DC can evaluate nodes' position very differently than BC; it may overestimate the importance of nodes belonging to isolated subgraphs (high DC-low BC) or underestimate the role of nodes acting as bridges between groups of nodes (low DC-high BC). On the other hand, high-degree nodes have better chances to be parts of the shortest paths linking node pairs. In our datasets, the two indices are found consistently highly correlated, in agreement with earlier studies [32], [47], [48] that report positive *Pearson* correlation between DC and BC over a wide range of networks such as random graphs and real-world complex networks.

Pagerank vs. Degree centrality. Another interesting result, that is immediately apparent from Figure 2, is the strong correlation between Pagerank and Degree centrality. Pagerank is principally defined for digraphs discriminating between incoming and outgoing connections at each node. For undirected general graphs, Grolmusz [49] shows that Pagerank is statistically close to the degree distribution but not identical. Furthermore, taking into account the aforementioned strong BC-DC correlation, a triangle-like schema emerges and may be of practical importance as it relates the only local index (*i.e.*, Degree) with globally-determined ones (*i.e.*, Pagerank and Betweenness centrality). Interestingly, significant positive correlation between these three indices (PG-DC-BC), with ρ values in $[0.66, 0.95]$ for all three index pairs, is also reported by Yan and Ding [50] over coauthorship real-world data (directed graphs).

Figure 3.a describes the monotonic increase of the PG-DC correlation with the damping factor d of PG. Pagerank [18] is often approached as the steady-state distribution of the frequency of visits to the network nodes by a random walker

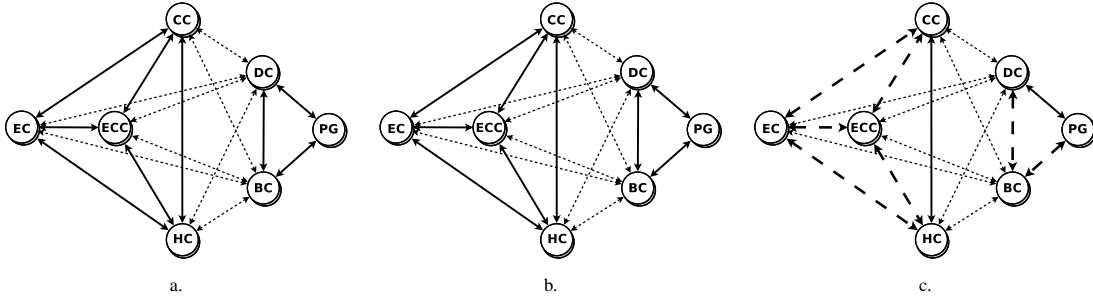


Fig. 2. Graph-based illustration for the average values of the Spearman (a), Kendall (b) coefficients and top-5% overlap (c) among centrality indices. In (a) and (b) solid bold and dashed plain lines denote coefficients in the intervals $[0.7-1]$, $[0.3-0.7]$, respectively. In (c), solid bold, dashed bold and dashed plain lines denote overlap value higher than 70%, between 40-70%, and lower than 40%, respectively. A special note involves the BC-CC and BC-HC pairs that exhibit increased values compared to this rule.

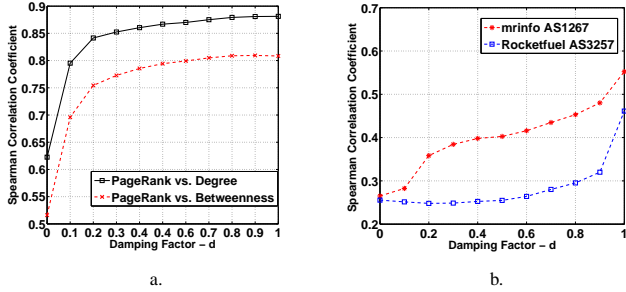


Fig. 3. a) Rank-correlation scaling as the Pagerank increasingly depends on DC and BC for AS1299. b) Rank-correlation between EC and PG as a function of the damping factor d for indicative ASes.

who each time either jumps towards another arbitrary network node with probability $(1-d)/N$, where N the cardinality of the network node set, or randomly follows an outbound link towards a neighboring node. As d increases the walker's long jumps get rarer and only 1-hop steps are feasible. Figure 3.a (dashed line) also shows similar association between the damping factor and the PG-BC ρ values.

Pagerank vs. Eigenvector centrality. PG, and EC centrality are the two spectral indices we experiment with. Both express the stationary probability of a random surfer to reside on some page while moving on the Web graph. Hence, one would expect some positive correlation between these indices. However, our results indicate the absence of such a relationship. A possible cause is that their actual interpretation differs as, contrary to EC, the PG Centrality utilizes the damping factor d to determine the ‘‘jump’’ probability. However, as a couple of indicative experiments suggest (Fig. 3.b), the rank correlation between the two metrics increases yet does not reach very high values as d moves to unity *i.e.*, the surfer moves only to neighboring pages. It seems then that d can only partially justify the poor PG-EC correlation strength; as the PG formula suggests (Table I) a node's (*i.e.*, Web page) PG rank value is evenly divided (L_u term) over its neighbors, which for the case of undirected graphs corresponds to its DC value. The fact that DC index is found to be weakly correlated with EC (Table II) can further distort any anticipated PG-EC

correlation.

Eccentricity vs. Closeness centrality. Another strong correlation that we observe in our correlation study involves the Eccentricity and Closeness centrality indices. Recalling the definitions of the two indices (ref. Table I), there is absolute positive ECC-CC correlation if it holds:

$$ECC(n_1) > ECC(n_2) \quad (1)$$

whenever

$$CC(n_1) > CC(n_2) \quad (2)$$

We can rewrite eq. 1 as

$$\max_{j \in V} d_{n_2, j} > \max_{j \in V} d_{n_1, j} \quad (3)$$

and eq. 2 as

$$\sum_{j \in V} d_{n_2, j} > \sum_{j \in V} d_{n_1, j} \quad (4)$$

Hence, the question becomes when the order in maximum index values (eq. 3) is also preserved for their averages (eq. 4) over a certain graph. This holds in several trivial graphs (*e.g.*, line graph, rectangular grid) but not in all graphs. One simple counterexample is the 4-node star network with a 2-node line graph attached to one of its leaf nodes (compare the two indices for the hub node and the leaf node, where the line graph is attached).

Additional remarks. There exist further centrality pairs yielding positive correlations, which are less straightforward to reason about. For instance, in our results, high rank correlation has been observed for pairs such as Eigenvector-Harmonic and Eigenvector-Closeness centrality. These findings seem consistent with previous results. Iyer *et al.* [51] have noticed that synthetic scale-free networks (whose degree distribution follows a power law, at least asymptotically) present moderate positive Pearson CC-EC correlation. Higher values ($r=0.61$) are reported for the case of networks with exponential degree distribution.

Elaborating more on this thread, we have tried to identify how the degree distribution relates to the EC-CC correlation. In Figure 4 left, we plot in log-log scale the degree distribution of a 411-node large AS out of the RocketFuel datasets, as a representative sample, with positive Pearson correlation be-

tween EC and CC ($r=0.65$). The straight-line points to power-law degree distribution suggesting that this may be beneficial for the positive correlation, as in [51]. On the other hand, the

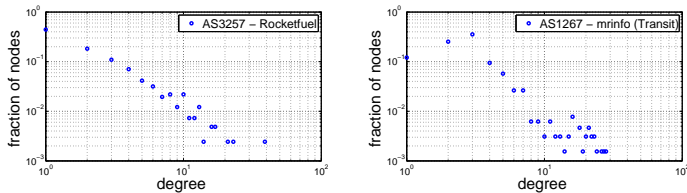


Fig. 4. Degree distribution for two indicative snapshots.

scale-free property is not a necessary condition for high EC-CC correlation. In Figure 4 right, the degree distribution of a 645-node large mInfo Transit AS clearly deviates from a power-law pattern, yet it features a considerably higher Pearson coefficient ($r=0.78$). Similar remarks hold for the EC-CC rank correlation over these snapshots (where we measure the corresponding Spearman $\rho_V=0.88$ for the former and $\rho_V=0.96$ for the latter one).

2) *Top-k percentage overlap over binary graphs*: So far, our correlation analysis has taken into account the full rankings produced by the seven centrality indices. We now focus our attention on the top-5% most central nodes identified by each index and investigate how large are the overlaps between different rankings. Our motivation for this set of experiments is the existence of network protocol instances that typically seek to exploit a small set of the top-central nodes [16]. Likewise, vulnerability studies of Internet graphs, as the one we carry out in Section IV, are concerned with the subset of most central nodes.

In Figure 2.c we show a summarizing graph-based illustration of the overlap scores among the seven centrality indices. The bold solid lines (e.g., between CC-HC) denote what we consider as high top-5% overlap between two centralities i.e., beyond 70%. The dashed solid lines (e.g., between EC-HC) reflect overlap values between 40-70%, whereas the dashed plain lines represent looser relations for the corresponding pairs. Additionally, figure 5 presents the average overlap of nodes over all ASes of each dataset for the most significant centrality pairs. On the one hand the overlap of some indices (such as BC-CC or HC-BC) appear to be highly sensitive to the considered topology, with differences that reach 40% across different datasets. On the other, all pairs that are strongly correlated in terms of full rankings in III-B1 appear to be more weakly associated in terms of overlap values⁵. Exceptions to that rule are the HC-BC and CC-BC pairs that represent a slight increase of the relation strength when passing from the rank correlation to the overlap measure. Overall, only two of the centrality index pairs combine high overlap values with strong full rank-correlation (see Figure 2.a): PG-DC and HC-CC, both exhibiting larger than 80% overlap in the top-5%

⁵The characterization retains a loose empirical meaning; essentially, the comparison between a correlation coefficient and the % overlap value is not straightforward.

node rankings they induce across all datasets, whereas all the other pairs hardly exceed the 60% value. This result should come as no surprise since rank correlation is determined over all network nodes rather than a subset of cardinality k .

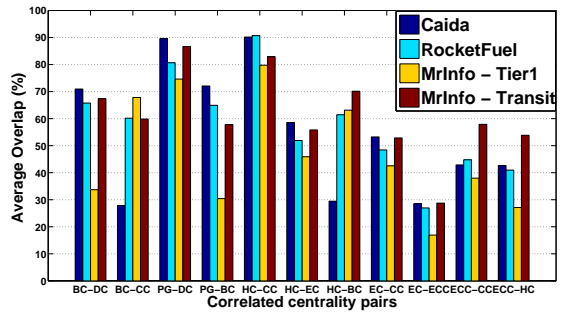


Fig. 5. Mean overlap (%) of the top-5% important nodes between centrality rankings over all ASes.

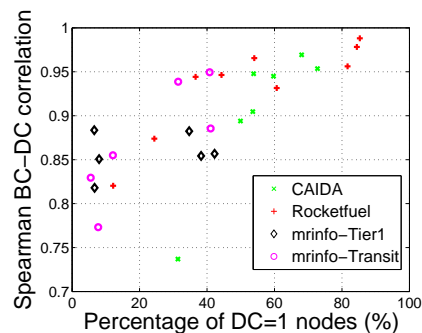


Fig. 6. Plot of the relation between the BC-DC rank correlation and the percentage of nodes with degree equal to one. (A pair of outlier values for the mInfo (Tier1) dataset have been omitted.)

TABLE III
RANK CORRELATION STRENGTH VS. OVERLAP (%) BETWEEN BC AND DC

Dataset-ID	BC-DC Spearman Coefficient	Top-5% Overlap	Fraction of nodes having DC=1
CAIDA-1557	0.95	53%	54%
RocketFuel-1239	0.96	85%	82%
MrInfo, Tier1-1239	0.86	54%	43%
MrInfo, Transit-3292	0.94	40%	32%

Let us look closer into the BC-DC pair. For these two indices, there is an apparent association between the nodes that are ranked in the last positions by the two indices; namely, nodes with the lowest DC value (i.e., DC=1) exhibit as well the lowest BC value (i.e., BC=0). Figure 6 illustrates how the number of nodes with DC=1 affects the rank correlation coefficients. It seems that (especially for the datasets of Caida and RocketFuel) the Spearman values between the considered indices increase with the number of DC=1 nodes. These nodes are expected to positively contribute to the DC-BC correlation as they also exhibit the lowest-ranked betweenness value (i.e., BC=0). At the same time, the ones with the top BC and DC values may not necessarily coincide as indicated

in Table III. The above results suggest that the high DC-BC correlation is mainly due to nodes of lowest ranks. This observation warns against the actual value of high Spearman rank correlation coefficients between two indices. On the other hand, the overlap measure does not suffer from similar biases. The repercussions of this will become clearer in the results of the Section IV experiments.

3) *Correlation/overlap results over capacitated graphs:* We have carried out a brief correlation study to identify how the node rankings generated by the indices, relate over the topology Zoo dataset. For determining the node rankings we had to carry out the centrality indices computations over weighted graphs. This was mainly a question of computing shortest paths over weighted graphs. Regarding the spectral indices, in the Topology Zoo experiments we only employ the EC index that lends to a straightforward extension over the weighted graphs (see paragraph II-A2). As such, we compute the Spearman correlation coefficients for the centrality pairs across all 18 snapshots. Table IV summarizes our results demonstrating the average and variance values for the measured coefficients, respectively. Those index pairs that were measured earlier to be strongly correlated over the binary graphs (*i.e.*, Figure 2.a), generally maintain similar relations over the capacitated Zoo networks. A relevant comment involves the BC-DC correlation which is again found high yet not as close to unity as before; ECC and EC appear in most cases highly correlated except for a few topologies that contribute to a high variance value for the coefficient average. Clearly, these results are shaped by both the topology and the link capacity values that are now taken into account for the corresponding index computations.

TABLE IV
SPEARMAN AVERAGES AND VARIANCE FOR THE TOPOLOGY ZOO DATASET

	BC	CC	DC	EC	HC	ECC
BC	1					
CC	0.68±0.01	1				
DC	0.75±0.01	0.85±0.02	1			
EC	0.59±0.03	0.94±0.01	0.79±0.04	1		
HC	0.68±0.01	0.98±0.01	0.87±0.01	0.95±0.01	1	
ECC	0.64±0.01	0.87±0.04	0.80±0.02	0.77±0.16	0.86±0.04	1

TABLE V
AVERAGE TOP-15% OVERLAP (%) FOR THE TOPOLOGY ZOO DATASET

	BC	CC	DC	EC	HC	ECC
BC	1					
CC	75.55	1				
DC	78.38	84.36	1			
EC	67.40	84.07	78.06	1		
HC	75.55	89.63	85.10	87.77	1	
ECC	69.99	77.91	73.62	71.24	73.09	1

In Table V we present our results for the overlap between the $k\%$ top central nodes averaged over the whole topology Zoo dataset. As their size is relatively small, we have chosen to set $k = 15\%$ in order to each time avail vectors of at least 5 nodes' size. Compared to the $topk$ overlap measured over the binary graphs, we have found the same index pairs to exhibit high values; one exception is the HC-DC pair which now appears of considerably high overlap. Still, we will see in

the experimentation section how these overlap values reflect on the (similar) effects of the corresponding node removals.

IV. CENTRALITY AND NETWORK VULNERABILITY

The correlation study yields a first indirect indication of how different centrality indices compare and whether they could be interchanged in the context of a network protocol or analysis that draws on node rankings. The ultimate reply to this question is, however, protocol/analysis-dependent. In this section, we seek to come up with a reply in the context of the network vulnerability to node failures. More specifically, we ask how much different are the conclusions about the network vulnerability when its most central nodes are removed in line with the rankings induced by the different centrality indices⁶.

The network vulnerability analysis is of interest to various parties. A potential attacker would like to know which centrality index can reveal the node set, whose removal has the the most significant impact on the network performance, so as to orchestrate the most effective attack. From the network operator's side, the dual aim is to identify and secure the most critical network nodes that, when shut-down by an attack, result in maximum network performance degradation. In this paper, we relate the term "performance" to fundamental connectivity and traffic capacity properties of the network rather than the scores achieved by specific protocols/applications. This way we get away with their engineering details that shape the end impact and place the emphasis on the network topologies as such.

A. Centrality-driven node removals and connectivity

Our study evaluates the impact of node removals on three different connectivity measures of the Internet graphs: (i) the size of the giant connected component; (ii) the total number of connected components in the graph; and (iii) the average shortest path length⁷ between all nodes. Experiments are carried out over the binary datasets described in the subsection III-A2.

Figure 7 presents a representative set of results showing the impact of centrality-driven node removals on the network connectivity. Experimental points correspond to removals up to 5% of the network size since the connectivity properties tend to stabilize thereafter. Apart from the three connectivity measures we also compute the Max/Min ratio (plotted in dashed line and measured on right Y axis); this is the fraction between the maximum and minimum value of the connectivity measure as obtained over all centrality indices. The Max/Min ratio essentially seeks to quantify the effectiveness loss in terms of network connectivity between the optimal and worst choice out of the considered indices.

⁶In this report, nodes are removed simultaneously after being ranked in order of decreasing centrality values. An alternative, lying at the core of what is often called *sequential* targeted attack strategy, is to recalculate the rankings of the residual nodes after each node removal. As intuitively expected and shown in [51]–[53] the impact of such sequential node removals upon network connectivity properties is more dramatic. Expanding our study to the sequential node removal case is straightforward.

⁷Shortest paths are computed only for node pairs residing in the same connected component.

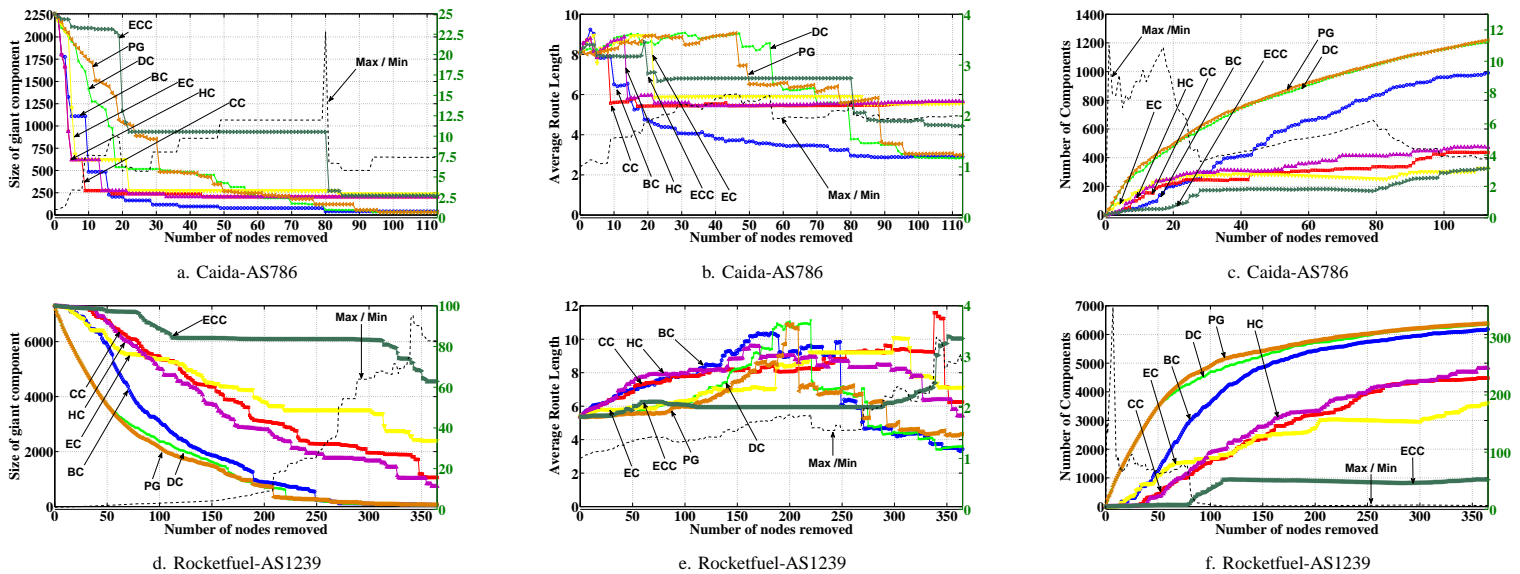


Fig. 7. Effects of node removals on three network connectivity measures *i.e.*, the size of the giant-connected component (a,d), the average path-length (b,e) and the number of components (c,f) for two indicative ASes.

In view of the reported correlation results, one may expect that any two highly rank-correlated indices should have similar impact over the network connectivity, when used to drive node removals. Interestingly, our results suggest that this is rarely the case for all three connectivity measures. In what follows we comment on the experimentation outcomes seeking to relate them to the earlier observed correlations; conclusions are mainly drawn with respect to four highly-correlated index pairs (*i.e.*, BC-DC, PG-DC, HC-CC and PG-BC) as well as a couple of weakly associated ones (*e.g.*, HC-BC or BC-CC).

1) *Size of giant connected component (GCC)*: The size of Giant Connected Component (GCC) reflects the number of nodes being able to communicate with each other. The only consistent result here involves the least effective index. As Figs. 7.a and .d suggest removing vertices as determined by the Eccentricity measure, has the minimum impact on GCC. All other indices expose more quickly the vulnerability of the network. Yet, we cannot identify any dominance relationship among them across all datasets. However, the behavior of certain pairs such as the HC-CC and PG-DC is in good agreement with the earlier observed strong associations, both in rank-correlation and top- k overlap (*i.e.*, ρ_v and ov_V higher than 0.85 and 85%, respectively); indeed, the corresponding curves in Figs 7.a and .d appear to be (partially) coincide or exhibiting small GCC size differences as nodes are removed. A closer look reveals that it is the top- k overlap between two indices, rather than their rank-correlation, that essentially determines how similar is the impact of the corresponding removals. A relevant example is the index of BC and DC over AS1239 which in Fig 7.d demonstrate highly dissimilar impact; their measured top-5% overlap does not exceed 68% while the Spearman ρ_v reaches 0.94.

Comparing the impact of the locally-determined, DC-

driven removal against the globally-determined BC-driven one, Holme *et al.* [52] showed that the two types are equally harmful over synthetic (scale-free) topologies, while a distinct real-world co-authorship network appears more vulnerable to BC-driven attack. In our broad dataset of real-world topologies we do not witness expressions of the latter effect; on the contrary, the local DC index occasionally turns out to have more dramatic impact than the global BC.

Overall, the concluding note here would be that *any two indices measured with high top- k overlap values would appear to cause exactly the same impact on the connected component for a certain sequence of node removals, and vice versa. The full-rank correlation values are not always in line with the experienced impact.*

2) *Average shortest path length*: Regarding the average shortest path length, there is no index that constantly exhibits the best or worst performance while all present a twofold behavior over every topology. First, the average path length increases and then, suddenly follows a fast decay (Figure 7.b and .e). This fluctuation seems to mainly depend on how fast the centrality-driven node removals lead to the total network fragmentation. Potentially, there exists an upper bound of node removals that permits the giant component to maintain a relatively large size before its connectivity has been significantly diminished. Consequently, as long as the largest connected component maintains a significant size, the node removals result in increasingly longer paths between its node pairs; when the network has been broken down to several small clusters, further removals tend to create single isolated nodes and therefore, decrease the average shortest path. Looking at how the correlation results predict the impact of removals, we notice that the highly associated indices in both rank-correlation and top- k overlap (*i.e.*, HC-CC, PG-DC) again have

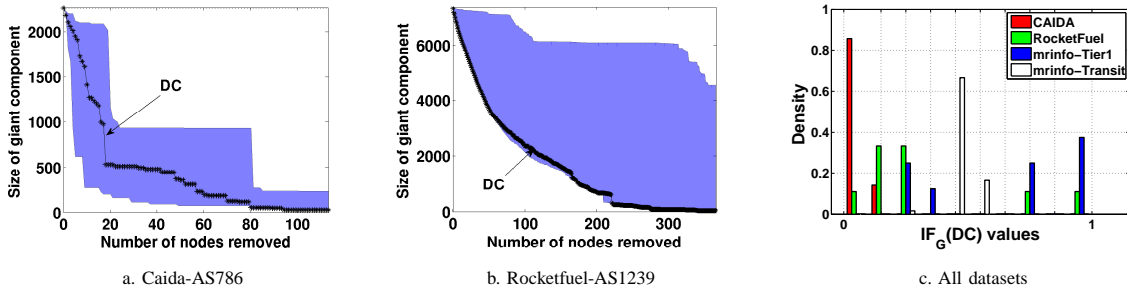


Fig. 8. a,b)Envelope plots of the DC-based node removal effects on the size of the giant-connected component for two indicative ASes. c) Empirical probability mass function of the $IF_G(DC)$ measured with respect to the size of the giant component.

similar impact, whereas those of slightly weaker association in at least one association metric (*i.e.*, BC-DC, PG-BC), may affect the average shortest path length in considerably different ways.

3) *Number of connected components*: As far as the the number of connected components is concerned, ECC is again found the dominant index in terms of the least effective removal (Figure 7.c and .f). According to the ECC notion [13], a node is central when its maximum distance to any other node is close to the radius of the graph. Hence, a node can exhibit a significantly low ECC value when only a few other nodes lie far away (from it) in the topology. This sensitivity makes ECC assigning less significance to nodes considered highly-central with respect to other indices. So when removing the top-5% ranked nodes we may not actually refer to those holding prominent network locations and this prevents the fast fragmentation of the topology. In sharp contrast, DC and PG are together the dominant in terms of effectively partitioning the topology, as their earlier observed high association values suggest. Interestingly, DC, a purely local index succeeds in removing nodes that play critical role in connectivity as opposed to the other global and more complex ones (except for PG). On the other hand, BC and DC which were also found strongly rank-correlated yet of weaker top- k overlap, cause different impact over the connected components. Removing vertices according to DC, the number of components increases constantly compared to the impact of the BC-driven node removals. This implies that the network connectivity mainly relies on strategic hub-nodes rather than bridge nodes that are typically of high BC.

4) *Local vs. global centrality indices*: Figure 7 clearly shows that the removal of the most central nodes may have a significantly varying impact depending on which centrality index is used to determine them. Conceptually, for each number k of removed nodes, one can identify best- and worst-case values, $m_{bc}(k)$ and $m_{wc}(k)$ respectively, for all three performance metrics plotted in Fig. 7. These values may be obtained by different centrality indices as the considered metric m changes and outline an envelope. Such envelopes define the shaded area in Figs 8.a,b. What we ask next is where in this envelope the metric values corresponding to the degree centrality, lie. Essentially, we would like to quantify how close

to the best-/worst-case is the impact of removals when directed by the single locally computable centrality index.

To this end, for each centrality index c , topology G , number of removed nodes k and performance metric $m(k; c)$ we define a normalized distance measure, hereafter called impact factor $IF_G(k; c)$ as:

$$IF_G(k; c) = \frac{|m(k; c) - m_{wc}(k)|}{|m_{bc}(k) - m_{wc}(k)|}$$

Note that depending on the metric, the worst-case value may coincide with the minimum or maximum value the metric gets over all indices. It is then straightforward to derive a topology-average measure of the impact factor as:

$$IF_G(c) = \frac{1}{|\mathcal{K}|} \sum_{k \in \mathcal{K}} \frac{|m(k; c) - m_{wc}(k)|}{|m_{bc}(k) - m_{wc}(k)|}$$

where \mathcal{K} is the set of k values considered in the evaluation. Clearly, both $IF_G(k; c), k \in \mathcal{K}$ and $IF_G(c)$ take values in $[0, 1]$. We are particularly interested in $IF_G(DC)$ and Figure 8.c plots the empirical probability mass function of the $IF_G(DC)$ values over all topologies of a given dataset, when the metric m is taken to be the size of the giant connected component. Despite its local nature, DC is proved in most cases to cause significant impact on the giant connected component. To which extent this impact approximates the most effective removal appears to depend on the underlying network topology. Over the CAIDA networks DC can closely approximate the most effective index while it seems to offer a less effective approximation over the Rocketfuel topologies. Finally, in the minfo (Tier-1) and (Transit) topologies, considerable mass appears for medium and high $IF_G(DC)$ values, respectively. This renders DC as an option of very low effectiveness for both datasets.

B. Centrality-driven node removals and traffic capacity

We now turn our attention to a much less investigated topic, the comparative impact of centrality-driven node removals on the network traffic serving capacity.

Such a task is not straightforward. One approach would be to consider a given traffic matrix, determining either the node pairs that exchange traffic only or the node pairs plus

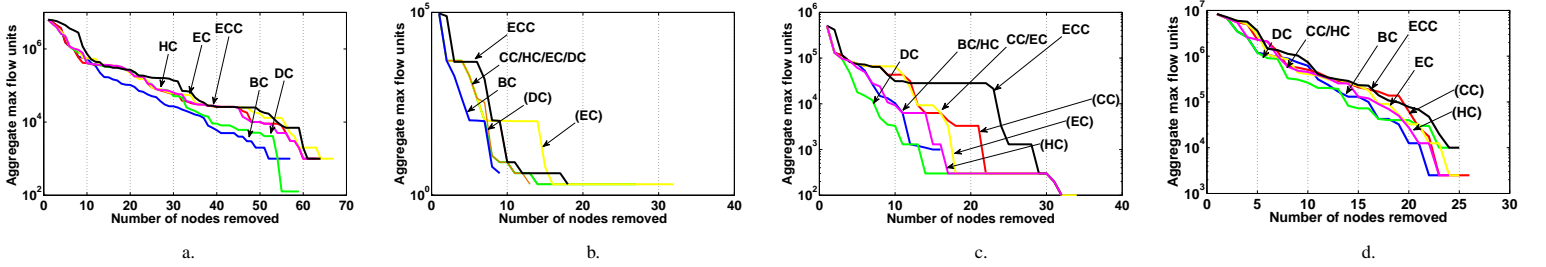


Fig. 9. Impact of node removal (in centrality-decreasing order) on the maximum flow the networks accommodate: (a) the Uninet I_{mean}, (b) Carnet, (c) Bren and (d) Geant. Wherever curves coincide, a single arrow identifier is used for multiple indices and when later on they become separated, each one is pointed with the corresponding index in parenthesis.

the average traffic loads that are (expected to be) served for each one of them. Then, the traffic-serving capacity of the network could be given by the solution of some version of the multicommodity flow (MCF) problem [12]. Yet doing so bears two significant challenges: First, the traffic demand matrix is rarely known a priori and often varies broadly over different time scales. Secondly, and most importantly, the MCF problem is an NP-complete problem [54], with the computational complexity raising fast with the number of commodities.

To overcome those limitations, we have taken a simpler approach and estimate the traffic serving capacity of the network as the sum of maximum flows over all network node pairs. Namely, we iterate over all node pairs and for each pair we solve an instance of the maximum flow problem, *i.e.*, compute the maximum traffic load that can be served by the network when only the particular pair transfers traffic across the network. Clearly, this sum is a (very) loose upper bound of the traffic load that can simultaneously be served by the network. However, it provides a traffic load-neutral measure of what can the network carry and how is this affected when a variable number of nodes is removed. For the solution of the the maximum flow problem we have employed the Edmonds-Karp algorithm [55] with a $O(V \cdot E^2)$ polynomial-time complexity (where V and E is the total number of nodes and edges, respectively).

1) *Experimentation methodology and results:* Our experimental study was carried out over the Zoo Internet topologies with capacitated links, described in Section III-A2. We remove nodes in decreasing order of centrality and measure the aggregate maximum flow over all node pairs.

The computed aggregate maximum flow over an indicative set of networks is plotted in Fig. 9. We have obtained similar results for the rest of the topology Zoo dataset (18 snapshots in total). The rate of aggregate max flow reduction with the fraction of removed nodes varies widely, as shown in Fig. 9. This results in high best- to worst-case flow values and wide envelopes, as shown in Fig. 10.a). Highly correlated index pairs, especially those with high top- k overlaps, impact the accommodated flow in similar ways (*i.e.*, intersection of corresponding curves). In particular, certain index pairs that have been earlier measured with high rank-correlation, and most notably overlap of the top central nodes, yield

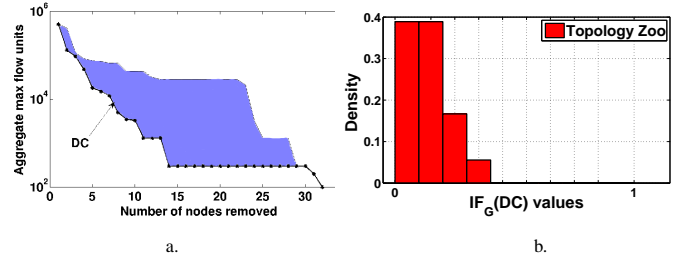


Fig. 10. a) Envelope plot of the DC-based node removal effects on the max flow in the Bren topology. b) Empirical probability mass function of the $IF_G(DC)$ measured with respect to the max flow the Topology Zoo dataset accommodates.

similar curves over a sequence of removals; for instance, the highly associated pairs of EC-CC, EC-HC and HC-CC (see Tables IV and V) are seen in Figs. 9.b and .c. Similar impact of BC- and DC-driver node removals has been reported over synthetic graphs (*i.e.*, Erdős-Rényi and small-world networks) in [56], yet in our case the impact of these two indices is typically different over the considered Internet snapshots. Finally, weakly correlated pairs such as EC-BC and ECC-BC, inline with intuition, yield well-separated aggregate flow curves.

On a positive note, when node removals are driven by the DC index, the resulting aggregate maximum flow in most cases of Fig. 9 is very close to the worst achieved over all indices. This is more clearly shown in the empirical probability mass function of the $IF_G(DC)$ measure in Fig. 10.b, whose mass is highly concentrated in (very) low values close to zero. On the contrary, the considered networks exhibit their highest resilience against the ECC-driven node removals. This behavior can be explained along the same arguments employed earlier, when discussing the impact of node removals on the connected components. Having a single node *i.e.*, the furthest one determine the ECC value may result in some of the most central nodes not being included in the top positions of the ECC ranking.

V. RELATED WORK

We group relevant work in literature along two threads:

Surveys and categorization of centrality indices: Our detailed survey of more than 30 different centrality indices

appears in [12]. Similar studies are rare in literature despite the extended use of centrality indices. One of the first relevant attempts dates back to 1979. Freeman reviewed several centrality indices that had been introduced by that time and reduced them down to three fundamental centrality notions, expressed by the degree, closeness and betweenness centrality [7]. More recently, Borgatti [38] introduced a typology of the different flows that may occur through a network and accordingly associated the various centrality measures with the flows that they are most appropriate for. Whereas the graph-theoretic review in [34] classifies centrality measures on the basis of the requirements posed by their calculation. Compared to these works, our approach reviews a great body of centrality indices, with very different origin and motivation, and seeks to classify them along multiple dimensions. At the same time we retain special interest for “engineering” properties such as the complexity related to the computation of the indices in distributed Internet environments.

Correlation of indices and use for network resilience studies: Likewise limited are the correlation studies of centrality indices. Two studies we are aware of compute linear correlation values between the two most well-known indices (*e.g.*, degree and betweenness centrality); the first employs a random network and a couple of real-world topologies with a single router-level snapshot [47], while the second presents experiments over three AS-level snapshots representing the same network along three consecutive years [48]. Neither of the two works assesses how the network is affected when different centrality indices are used to direct intelligent attacks. On the other hand, there is significantly richer literature with respect to attacks that are directed towards the most central network nodes. Most of them concern synthetic graphs and the attack impact is measured through purely topological measures. The scale free topologies have been found vulnerable to high-degree nodes [57]. In [52], attacks target the high-degree and -betweenness nodes in a real-world AS-level topology. The two attacks are found equally harmful in terms of the inverse geodesic length and the number of connected components in the residual network. More recently, the work in [58] considers both random node failure and centrality-driven node attacks in the context of a more general network topological robustness framework. Experimenting with families of random graphs, power grids, railway and co-authorship networks the authors show that many centrality indices drive removals of similar impact and that DC and EC relate to the most harmful ones.

Similar experimental results on the vulnerability of the Internet router-level graphs to centrality-driven node attacks seem to be missing, especially when the studied network property is the accommodated traffic. In an earlier work [32], we have related the correlation values between socio- and egocentric BC computations with the effectiveness of the local centrality-driven content search over ISP networks. Here, we generalize the approach by considering an extended set of centrality indices/topologies and adding traffic-carrying capacity measures to the network resilience context.

VI. CONCLUSIONS

Our paper has iterated on the broad variety of indices that embody and quantify *point centrality*, a popular concept borrowed from the Social Network Analysis and increasingly used in information network analysis and protocol design. Our starting point is a novel classification scheme that attempts to systematically characterize more than thirty indices proposed over the last sixty years by sociologists, physicists, and, to a lesser extent, biologists and computer scientists.

We have then chosen the seven most popular and representative of these indices and derived how they rank the nodes of more than 40 router-level topologies. We have found high rank correlations of certain index pairs such as DC-BC and DC-PG that persist across all four topology datasets we experiment with. Yet a significant part of the high full rank correlation is due to the nodes that are ranked last (*e.g.*, DC=1, BC=0) so that the association weakens when we consider the overlap between the sets of the top-5% most central nodes only. In several cases, these findings stand in agreement with what has been reported in literature for other types of real and synthetic networks.

Finally, we have experimentally assessed the impact of removing the most central nodes of the network, as determined by each index, on its *connectivity* properties and *traffic-serving capacity*. As expected, it is the top-5% overlap rather than the full rank correlation that can predict more accurately when the node removals that are determined by two different indices have similar impact on the network. This is a warning against the widespread use of full rank correlation as a proxy for the “equivalence” of two indices. In general, the use of different indices for the choice of to-be-removed nodes varies significantly the impact of the network. Whereas ECC is consistently the index with the least impact, the indices that induce the more dramatic changes on the network performance change with the topology and performance measure. However, and less intuitively, the single index that can be computed through local-only information (*i.e.*, DC) appears to approximate closely the worst-case impact on the network traffic capacity.

One hint for vulnerability analysis out of these results is that the added complexity of global indices may be escaped when we want an estimate of what is the worst-case impact on the network. A second hint towards attackers (network operators) is that it might be worth considering attacking (resp. better defending) a set of nodes that results from mixing the rankings of two indices, *e.g.*, one local and one global. In this case, the top-*k* overlap measure between the two ranking could serve as criterion for the efficiency of this mixing: if it is high, then there is little more to gain by mixing; if it is low, then mixing might generate a node set, whose removal affects the network even more dramatically. This is a direction that we are currently investigating.

REFERENCES

- [1] S. Wasserman and K. Faust, *Social network analysis: Methods and applications*. Cambridge Univ Pr, 1994.
- [2] A. Bavelas, "A mathematical model of Group Structure," *Human Organizations*, vol. 7, pp. 16–30, 1948.
- [3] L. Katz, "A new status index derived from sociometric data analysis," *Psychometrika*, vol. 18, pp. 34–43, 1953.
- [4] M. Beauchamp, "An improved index of centrality," *Behavioral Science*, vol. 10, pp. 161–163, 1965.
- [5] J. Anthonisse, "The rush in a directed graph." *Technical Report BN9/71, Stichting Mahtematisch Centrum*, Amsterdam, 1971.
- [6] G. Sabidussi, "The centrality index of a graph," *Psychometrika*, vol. 31, pp. 581–603, 1966.
- [7] L. C. Freeman, "Centrality in social networks: Conceptual clarification," *Social Networks*, vol. 1, no. 3, pp. 215–239.
- [8] P. Bonacich, "Power and centrality: A family of measures," *American Journal of Sociology*, vol. 92, no. 5, pp. 1170–1182, 1987.
- [9] E. M. Daly and M. Haahr, "Social network analysis for information flow in disconnected delay-tolerant manets," *IEEE Trans. Mob. Comput.*, vol. 8, no. 5, pp. 606–621, 2009.
- [10] W. K. Chai, D. He, I. Psaras, and G. Pavlou, "Cache "less for more" in information-centric networks," in *Proc. of the 11th IFIP Networking*, Prague, Czech Republic, May 2012.
- [11] A.-L. Barabasi, "Linked: The new science of networks," Perseus Pub., 2002.
- [12] G. Nomikos, "Point centrality indices and ISP network vulnerability," September 2013, MSc Thesis, Dept. of Informatics & Telecom., UoA. [Online]. Available: <http://anr.di.uoa.gr/index.php/theses>
- [13] P. Hagea and F. Harary, "Eccentricity and centrality in networks," *Social Networks*, vol. 17, no. 1, pp. 57–63, Jan. 1995.
- [14] M. J. Newman, "A measure of betweenness centrality based on random walks," *Social Networks*, vol. 27, no. 1, pp. 39 – 54, 2005.
- [15] A. Tizghadam and A. Leon-Garcia, "On traffic-aware betweenness and network criticality," in *INFOCOM IEEE Conference on Computer Communications Workshops*, 2010, 2010, pp. 1–6.
- [16] P. Pantazopoulos, M. Karaliopoulos, and I. Stavrakakis, "Centrality-driven scalable service migration," in *23rd International Teletraffic Congress (ITC'11)*, San Francisco, USA, Sept. 2011.
- [17] L. C. Freeman, "A set of measures of centrality based on betweenness," *Sociometry*, vol. 40, no. 1, pp. 35–41, 1977.
- [18] L. Page, S. Brin, R. Motwani, and T. Winograd, "The pagerank citation ranking: Bringing order to the web," Stanford University, Technical Report, 1998.
- [19] A. Barrat, M. Barthélemy, R. Pastor-Satorras, and A. Vespignani, "The architecture of complex weighted networks," *Proceedings of the National Academy of Sciences of the United States of America*, vol. 101, no. 11, pp. 3747–3752, Mar. 2004.
- [20] U. Brandes, "On variants of shortest-path betweenness centrality and their generic computation," *Social Networks*, vol. 30, no. 2, 2008.
- [21] M. E. J. Newman, "Analysis of weighted networks," *Phys. Rev. E*, vol. 70, no. 5, p. 056131, Nov. 2004.
- [22] W. Xing and A. Ghorbani, "Weighted pagerank algorithm," in *In Proc. Second Annual Conference on Communication Networks and Services Research*, May 2004, pp. 305 – 314.
- [23] X. Liu *et al.*, "Co-authorship networks in the digital library research community," *Inf. Process. Manage.*, vol. 41, no. 6, pp. 1462–1480, 2005.
- [24] J. Bollen, M. A. Rodriguez, and H. Van de Sompel, "Journal status," *Scientometrics*, vol. 69, no. 3, pp. 669–687, 2006.
- [25] V. Kostakos, "Temporal graphs," *Physica A: Statistical Mechanics and its Applications*, vol. 388, no. 6, pp. 1007–1023, 2009.
- [26] B. B. Xuan, A. Ferreira, and A. Jarry, "Computing shortest, fastest, and foremost journeys in dynamic networks," *International Journal of Foundations of Computer Science*, vol. 14, no. 2, pp. 267–285, 2003.
- [27] S. Merugu, M. Ammar, and E. Zegura, "Routing in Space and Time in Networks with Predictable Mobility," *Technical Report, Georgia Institute of Technology*, 2004. [Online]. Available: <https://smartech.gatech.edu/handle/1853/6492>
- [28] A. Orda and R. Rom, "Shortest-path and minimum-delay algorithms in networks with time-dependent edge-length," *Journal of the ACM*, vol. 37, pp. 607–625, 1990.
- [29] J. Tang, M. Musolesi, C. Mascolo, V. Latora, and V. Nicosia, "Analysing information flows and key mediators through temporal centrality metrics," in *Proceedings of the 3rd Workshop on Social Network Systems*, ser. SNS '10. New York, NY, USA: ACM, 2010, pp. 3:1–3:6.
- [30] H. Kim and R. Anderson, "Temporal node centrality in complex networks," *Physical Review E*, vol. 85, 026107 (2012).
- [31] L. C. Freeman, "Centered graphs and the structure of ego networks," *Mathematical Social Sciences*, no. 3, pp. 291–234, 1982.
- [32] P. Pantazopoulos, M. Karaliopoulos, and I. Stavrakakis, "On the local approximations of node centrality in internet router-level topologies," in *the 7th IFIP IWSOS, Palma de Mallorca, Spain.*, May 2013.
- [33] D. S. Sade, "Sociometrics of Macaca Mulatta III: n-path centrality in grooming networks," *Social Networks*, vol. 11, no. 3, pp. 273–292, 1989.
- [34] S. Borgatti and M. Everett, "A Graph-theoretic perspective on centrality," *Social Networks*, vol. 28, no. 4, pp. 466–484, Oct. 2006.
- [35] P. Bonacich, "Simultaneous group and individual centralities," *Social Networks*, vol. 13, no. 2, pp. 155 – 168, 1991.
- [36] R. Moxley and N. Moxley, "Determining point-centrality in uncontrived social networks," *Sociometry*, vol. 37, no. 1, pp. 122–130, Mar. 1974.
- [37] T. Høivik and N. P. Gleditsch, "Structural parameters of graphs: A theoretical investigation," *Quantitative Sociology*, pp. 203–223, Academic Press, New York, 1975.
- [38] S. P. Borgatti, "Centrality and network flow," *Social Networks*, no. 27, pp. 55–71, 2005.
- [39] Y. Rochat, "Closeness centrality extended to unconnected graphs: The harmonic centrality index," in *proc. of Applications of Social Network Analysis*, Zurich, Switzerland (2009).
- [40] P. Hui, J. Crowcroft, and E. Yoneki, "Bubble rap: Social-based forwarding in delay-tolerant networks," *IEEE Trans. Mob. Comput.*, vol. 10, no. 11, pp. 1576 –1589, nov. 2011.
- [41] L. A. Adamic *et al.*, "Search in power-law networks," *Physical Review E*, vol. 64, no. 4, Sep. 2001.
- [42] N. T. Spring *et al.*, "Measuring ISP topologies with rocketfuel." *IEEE/ACM Trans. Netw.*, vol. 12, no. 1, pp. 2–16, 2004.
- [43] The CAIDA UCSD Macroscopic Internet Topology Data Kit (ITDK) - [ITDK 2011-10]. [Online]. Available: <http://www.caida.org/data/active/internet-topology-data-kit/>
- [44] J.-J. Pansiot *et al.*, "Extracting intra-domain topology from mrinfo probing," in *Proc. PAM*, Zurich, Switzerland, April 2010.
- [45] R. M. Karp and R. E. Tarjan, "Linear expected-time algorithms for connectivity problems (extended abstract)," in *ACM STOC '80*, Los Angeles, California, 1980, pp. 368–377.
- [46] S. Knight, H. X. Nguyen, N. Falkner, R. A. Bowden, and M. Roughan, "The internet topology zoo." *IEEE Journal on Selected Areas in Communications*, vol. 29, no. 9, pp. 1765–1775, 2011.
- [47] C.-Y. Lee, "Correlations among centrality measures in complex networks." [Online]. Available: <http://arxiv.org/abs/physics/0605220>
- [48] A. Vázquez *et al.*, "Large-scale topological and dynamical properties of the internet," *Phys. Rev. E*, vol. 65, no. 6, p. 066130, Jun 2002.
- [49] V. Grolmusz, "A note on the pagerank of undirected graphs," May 2012. [Online]. Available: <http://arxiv.org/abs/1205.1960>
- [50] E. Yan and Y. Ding, "Applying centrality measures to impact analysis: A coauthorship network analysis," *J. Am. Soc. Inf. Sci. Technol.*, vol. 60, no. 10, pp. 2107–2118, Oct. 2009.
- [51] I. Swami, K. Timothy, S. Bala, and W. Zhen, "Attack robustness and centrality of complex networks," *PLoS ONE*, vol. 8, no. 4, April 2013. [Online]. Available: [doi:10.1371/journal.pone.0059613](https://doi.org/10.1371/journal.pone.0059613)
- [52] P. Holme, B. J. Kim, C. N. Yoon, and S. K. Han, "Attack vulnerability of complex networks," *Phys. Rev. E*, vol. 65, no. 5, May 2002.
- [53] L. Dall'Asta, A. Barrat, M. Barthélemy, and A. Vespignani, "Vulnerability of weighted networks," *J. Stat. Mech.*, p. P04006, 2006.
- [54] S. Even, A. Itai, and A. Shamir, "On the Complexity of Timetable and Multicommodity Flow Problems," *SIAM Journal on Computing*, vol. 5, no. 4, pp. 691–703, 1976.
- [55] J. Edmonds and R. M. Karp, "Theoretical improvements in algorithmic efficiency for network flow problems," *J. ACM*, vol. 19, no. 2, Apr. 1972.
- [56] I. Mishkovski *et al.*, "Vulnerability assessment of complex networks based on optimal flow measurements under intentional node and edge attacks," in *Proc. of ICT Innovations 2009*. Springer, pp. 167–176.
- [57] R. Albert, H. Jeong, and A.-L. Barabasi, "Error and attack tolerance of complex networks," *Nature*, vol. 406, no. 6794, pp. 378–382, Jul. 2000.
- [58] S. Trajanovski *et al.*, "Robustness envelopes of networks," *Journal of Complex Networks*, 2013. [Online]. Available: <http://comnet.oxfordjournals.org/content/early/2013/03/26/comnet.cnt004>

APPENDIX

A. Employed Internet router-level Topologies

In Tables VI and VII we present basic information about the network topologies employed for our experiments. The four datasets of the former table contain binary graphs whereas the later table contains capacitated graphs used mainly for the experimentation with the traffic serving capacity.

TABLE VI
PROPERTIES OF THE INTRA-DOMAIN ISP TOPOLOGIES

Dataset	ISP(AS no.)	<Clust. Coeff. >	Diameter	Size
Mrinfo (Tier-1)	Global Crossing(3549)	0.546	10	76
	-/-	0.479	9	100
	NTTC-Gin(2914)	0.307	11	180
	Sprint(1239)	0.298	12	216
	Level-3(3356)	0.169	25	378
	-/-	0.149	28	436
	Sprint(1239)	0.287	16	528
	-/-	0.251	13	741
	JanetUK(786)	0.132	14	336
	Mrinfo (Transit)	lunet(1267)	0.246	11
-/-	0.231	12	645	
-/-	0.038	13	711	
Telecom Italia(3269)	0.037	13	995	
TeleDanmark(3292)	0.058	15	1240	
Rocket Fuel	VSNL(4755)	0.263	6	41
	Ebone(1755)	0.115	13	295
	Tiscali(3257)	0.028	14	411
	Exodus(3967)	0.273	14	353
	Telstra (1221)	0.015	15	2515
	Sprint(1239)	0.022	13	7303
	Level-3(3356)	0.097	10	1620
	AT&T(7018)	0.005	14	9418
	Verio (2914)	0.071	15	4607
	UUNet(701)	0.012	15	18281
CAIDA	COGENT/PSI(174)	0.062	32	14413
	LDCoNet(15557)	0.021	40	6598
	TeliaNet(1299)	0.037	13	3820
	ChinaTelecom(4134)	0.083	19	81121
	FUSE-NET(6181)	0.018	10	1831
JanetUK(786)	0.031	24	2259	

TABLE VII
PROPERTIES OF THE CAPACITATED IP-LEVEL ZOO TOPOLOGIES

Network	Geo Location	Date of snapshot	Diameter	Size
Janet Lense	UK	1/2011	4	20
Belnet I	Belgium	2003	3	23
Belnet II	Belgium	2006	3	23
Geant	cross-Europe	2009	7	34
Niif	Hungary	5/2009	7	36
Bren	Bulgaria	10/2010	8	37
Myren	Malaysia	3/2011	4	37
Kentman	Kent, UK	1/2011	6	38
Switch L3	Switzerland	2011	6	42
Renater	France	2010	9	43
Sanet	Slovakia	2008	13	43
Carnet	Croatia	8/2010	6	44
Uninett L_min	Norway	2011	9	69
Uninett L_max	-/-	-/-	-/-	69
Uninett L_mean	-/-	-/-	-/-	69
Uninett II_min	-/-	2010	9	74
Uninett II_max	-/-	-/-	-/-	74
Uninett II_mean	-/-	-/-	-/-	74

B. Averages of Kendall coefficients per dataset

As the graph representation shows (in Figure 2.b), the Kendall correlation values appear to be roughly similar to the Spearman ones; we have identified as dominant the same centrality pairs with the ones captured by the Spearman coefficient. However, a closer inspection on the absolute Kendall values of Table VIII shows a weaker dependence among the metrics; a somewhat looser relationship is therefore revealed

among the centrality indices than what the Spearman values may suggest.

TABLE VIII
AVERAGES OF KENDALL COEFFICIENTS FOR ALL DATASETS

	CC	HC	EC	ECC	DC	BC	PG	dataset
CC	1							CAIDA
	1							Rocketfuel
	1							Mrinfo-Tier1
	1							Mrinfo-Transit
HC	0.96	1						-/-
	0.91	1						-/-
	0.83	1						-/-
	0.92	1						-/-
EC	0.82	0.84	1					-/-
	0.66	0.68	1					-/-
	0.54	0.55	1					-/-
	0.72	0.74	1					-/-
ECC	0.73	0.72	0.71	1				-/-
	0.60	0.56	0.48	1				-/-
	0.66	0.55	0.42	1				-/-
	0.77	0.75	0.62	1				-/-
DC	0.22	0.22	0.23	0.22	1			-/-
	0.38	0.43	0.35	0.32	1			-/-
	0.33	0.47	0.36	0.25	1			-/-
	0.38	0.42	0.38	0.38	1			-/-
BC	0.22	0.22	0.21	0.22	0.83	1		-/-
	0.35	0.39	0.30	0.30	0.87	1		-/-
	0.37	0.47	0.22	0.30	0.60	1		-/-
	0.40	0.44	0.35	0.38	0.77	1		-/-
PG	0.01	0.02	0.03	-0.01	0.73	0.64	1	-/-
	0.16	0.20	0.09	0.14	0.72	0.66	1	-/-
	0.22	0.33	0.20	0.18	0.80	0.60	1	-/-
	0.27	0.30	0.24	0.27	0.82	0.74	1	-/-

C. Averages of Top-k overlap values per dataset

Next we present the top-5% overlap value between each index pair, averaged over all snapshots of the CAIDA, Rocketfuel, mrinfo-Tier-1 and -Transit datasets.

TABLE IX
AVERAGES OF TOP-5% OVERLAP (%) FOR ALL DATASETS

	CC	HC	EC	ECC	DC	BC	PG	dataset
CC	1							CAIDA
	1							Rocketfuel
	1							Mrinfo-Tier1
	1							Mrinfo-Transit
HC	90.1	1						-/-
	90.7	1						-/-
	79.8	1						-/-
	82.9	1						-/-
EC	53.2	58.6	1					-/-
	48.4	51.9	1					-/-
	42.5	45.9	1					-/-
	52.8	55.8	1					-/-
ECC	28.5	42.6	28.5	1				-/-
	26.9	40.9	27.0	1				-/-
	33.9	27.2	26.9	1				-/-
	28.8	53.9	32.0	1				-/-
DC	28.9	30.8	24.1	28.7	1			-/-
	57.4	62.1	46.6	29.9	1			-/-
	35.4	44.4	50.8	10.5	1			-/-
	42.0	53.9	39.9	32.6	1			-/-
BC	27.8	29.4	22.5	25.8	70.9	1		-/-
	60.1	61.4	32.3	34.7	65.8	1		-/-
	67.8	63.1	30.1	34.7	33.8	1		-/-
	59.8	70.1	40.9	44.8	67.3	1		-/-
PG	26.4	27.9	22.9	25.6	89.6	72.1	1	-/-
	46.6	50.8	35.2	20.7	80.7	64.9	1	-/-
	29.5	39.7	39.3	10.8	75.0	30.4	1	-/-
	33.0	44.8	38.3	25.6	86.7	57.8	1	-/-